

# Robust intensification of hydroclimatic intensity over East Asia from multi-model ensemble regional projections

Eun-Soon Im<sup>1</sup> · Yeon-Woo Choi<sup>2</sup> · Joong-Bae Ahn<sup>2</sup> 

Received: 14 February 2016 / Accepted: 14 June 2016 / Published online: 27 June 2016  
© The Author(s) 2016. This article is published with open access at Springerlink.com

**Abstract** This study assesses the hydroclimatic response to global warming over East Asia from multi-model ensemble regional projections. Four different regional climate models (RCMs), namely, WRF, HadGEM3-RA, RegCM4, and GRIMs, are used for dynamical downscaling of the Hadley Centre Global Environmental Model version 2–Atmosphere and Ocean (HadGEM2-AO) global projections forced by the representative concentration pathway (RCP4.5 and RCP8.5) scenarios. Annual mean precipitation, hydroclimatic intensity index (HY-INT), and wet and dry extreme indices are analyzed to identify the robust behavior of hydroclimatic change in response to enhanced emission scenarios using high-resolution (12.5 km) and long-term (1981–2100) daily precipitation. Ensemble projections exhibit increased hydroclimatic intensity across the entire domain and under both the RCP scenarios. However, a geographical pattern with predominantly intensified HY-INT does not fully emerge in the mean precipitation change because HY-INT is tied to the changes in the precipitation characteristics rather than to those in the precipitation amount. All projections show an enhancement of high intensity precipitation and a reduction of weak intensity precipitation, which lead to a possible shift in hydroclimatic regime prone to an increase of both wet and dry extremes. In general, projections forced by the RCP8.5 scenario tend to produce a much stronger response than do those by the

RCP4.5 scenario. However, the temperature increase under the RCP4.5 scenario is sufficiently large to induce significant changes in hydroclimatic intensity, despite the relatively uncertain change in mean precipitation. Likewise, the forced responses of HY-INT and the two extreme indices are more robust than that of mean precipitation, in terms of the statistical significance and model agreement.

## 1 Introduction

A series of assessments of the Intergovernmental Panel on Climate Change (IPCC) has induced growing scientific consensus that global warming due to anthropogenic forcing can manifest itself in regional- or local-level climate change in a highly nonlinear way (IPCC 2013). A significant body of research has focused on identifying the role of human-induced greenhouse gases (GHGs) in observed climate change (e.g., Min et al. 2011; Willett et al. 2007) and the enhancement of the reliability of future climate projections in response to various scenarios of future GHG emissions (e.g., Freychet et al. 2015; Fischer et al. 2014; Kendon et al. 2008). Based on the many studies projecting future climate, climate models tend to show a robust pattern of their forced response to a certain level of global warming (Fischer et al. 2014). For example, models agree on the intensification of heavy precipitation along with rising temperature in global average quantities, but disagree about the location and degree of increase (Fischer et al. 2014; Giorgi et al. 2011; Lau et al. 2013). From a broad sense of the thermodynamic perspective, hydroclimatic intensity is expected to become higher under global warming because of an increase in atmospheric moisture holding capacity of approximately 7 % for each 1 K increase in temperature, which is regulated by the Clausius–Clapeyron (C–C) relationship (Allen and Ingram 2002; Held

---

✉ Joong-Bae Ahn  
jbahn@pusan.ac.kr

<sup>1</sup> Singapore-MIT Alliance for Research and Technology (SMART), Center for Environmental Sensing and Modeling (CENSAM), Singapore, Singapore

<sup>2</sup> Division of Earth Environmental System, Pusan National University, Jangjeon 2-dong, Geumjeong-gu, Busan 609-735, South Korea

and Soden 2006; Giorgi et al. 2011; Chou et al. 2012; Endo and Kitoh 2014). Although this constraint could support the robust behaviors in terms of global average quantities, it seems to be often overwhelmed by local processes and natural variability in the process of precipitation formation at the regional scale. Therefore, the geographical patterns and magnitude of changes in the hydrologic cycle remain uncertain and suffer from statistical insignificance and a lack of model agreement. The magnitude and direction of changes in precipitation characteristics (i.e., intensity and frequency) that determine the hydrology cycle show high sensitivity at relatively smaller areas, depending on the model details, emission forcings, and target periods (e.g., Srivastara and Delsole 2014).

Due to coarse model resolution that prevents adequate representation of the effect of local-to-regional-scale forcings (e.g., complex topography and land surface characteristics) (Giorgi et al. 2009), global climate models (GCMs) suffer limitations in simulating regional climate in terms of heterogeneity and extremes (Lau et al. 2013; Wu et al. 2015), especially in the case of East Asia's monsoon climate. East Asia, including the Korean peninsula, is considered to be vulnerable to global warming (e.g., Im et al. 2008; Min et al. 2015) and to be dominated by advantages in climate simulations with higher resolution (e.g., Wu et al. 2015; Gao et al. 2006, 2012; Lee and Hong 2014; Niu et al. 2015). As part of an effort to improve climate projections, several previous studies have attempted to perform dynamical downscaling for the customized fine-scale climate projections over the Korean peninsula and the surrounding region (Oh et al. 2014; Lee et al. 2013; Lee and Hong 2014; Hong and Ahn 2015; Im et al. 2012a,b, 2015). However, such studies were mostly conducted individually based on a single model under different configurations. Hence, comprehensive assessment or inter-comparison has not been done within a well-organized framework. Although only a few studies have recently assessed the multi-regional climate model (RCM) projections based on the Coordinated Regional Climate Downscaling (CORDEX, Giorgi 2009) East Asia experiment, the standard resolution (50 km) of the CORDEX configuration remains insufficient to capture complicated physiographical features whose effect is significant in the weather and climate system over the Korean peninsula (Im et al. 2015). As the next step of CORDEX, the national downscaling project of Korea was performed with the aim of producing fine-scale (12.5 km) multi-model ensemble projections focusing on the Korean peninsula. This project is designed to perform dynamical downscaling using different RCMs but with the same driving fields (HadGEM2-AO (Hadley Centre Global Environmental Model version 2–Atmosphere and Ocean)) forced by the representative concentration pathway (RCP; Moss et al. 2010) scenarios of future emissions. These downscaled datasets using multiple RCMs achieved by coordinated collaboration are valuable, offering a good opportunity to analyze the multi-

model ensemble. There is general agreement that multi-model ensemble enhances the performance of present climate simulation and the reliability of future climate projection compared to a single model (IPCC 2013; Tebaldi and Knutti 2007; Knutti et al. 2010; Weigel et al. 2010; Deque et al. 2007; Pfeifer et al. 2015). However, the best way to combine the multi-model projections remains controversial and challenging. The combination of various projections from different models can be categorized as either “unweighted average” or “weighted average.” The simplest way of constructing a multi-model ensemble is to average out all participant models with equal weighting. Regardless of single model skill in simulating present climate, each model is equally weighted, assuming that individual model biases will partly cancel (Knutti et al. 2010). On the other hand, sophisticated approaches can be considered for applying different weights to individual models based on their performance measured by the distance from the historical observation. Various statistical techniques are used to determine optimum weighting. For example, the Bayesian method is applied to produce weighted ensemble average based on the integrated skill of each model (e.g., Min and Hense 2006), whereas the reliability ensemble average (REA) is proposed as the combination of model bias estimated from present climate simulation and inter-model agreement in the future projection (e.g., Giorgi and Mearns 2003). These studies argue that the weighted average shows better performance than does the arithmetic ensemble mean. However, the several drawbacks of these approaches do not support the superiority of optimum weighting over equal weighting. The first limitation is to assume that the relation between the training period (e.g., twentieth century) and the applied future period (e.g., late twenty-first century) will remain stationary (Tebaldi and Knutti 2007), which might not be true in nature. Next, it is very difficult to determine the appropriate weighting for an individual model. An essential prerequisite for optimum weighting is based on the evaluation of the model skill in simulating present climate. Since the model performance is very dependent on the particular period and region, the variables selected, and the observational data used, it is not possible to clearly distinguish or evaluate the model skill in a comprehensive and balanced way with accurate knowledge of not only single model skill but also relative contributions of the joint model error (Weigel et al. 2010). Furthermore, we cannot guarantee that the model with optimal performance in the present climate will maintain its optimization in the future. For example, a certain parameterization that works well under the current climate condition may become less effective or less appropriate in a warmer climate regime (Weigel et al. 2010). Therefore, in spite of potential gains by optimum weighting, equal weighting may be the safer and more transparent way to combine models (Weigel et al. 2010), and it is the most common approach adopted in many studies dealing with multi-model ensemble, including a series

of IPCC assessment reports. In this study, we apply equal weighting for the ensemble average from four regional climate projections, obtained from dynamical downscaling of the HadGEM2-AO global projection using the following four different RCMs: WRF, HadGEM3-RA, RegCM4, and GRIMs.

Uncertainties in regional climate projection based on dynamical downscaling arise from various sources, mostly referred to as anthropogenic emission forcing, GCM configuration, RCM configuration, and internal variability (Deque et al. 2007; Giorgi et al. 2009). In the present study, uncertainty means the spread measured by inter-model difference, which is somewhat different from the meaning used in short-term forecasting which is traditionally measured by the distance between the actual value to be predicted and its prediction (Deque et al. 2007). Deque et al. (2007) demonstrated using a set of RCM projections that the contribution of different sources to uncertainty varies according to the field, region, and season. More specifically, summer precipitation dominated by local process (e.g., convection) is more influenced by the choice of the RCM than boundary forcing (e.g., GCM), whereas temperature is more dependent on the uncertainty in GCM. The present study focuses on the uncertainty introduced by RCM configurations, highlighting the importance of inter-model agreement in assigning confidence to the future changes of hydroclimate intensity.

All the RCM simulations used in this study clearly suffer from some deficiencies, even though the performance of each individual RCM is optimized over our target region through various sensitivity experiments. Statistical adjustment can be an option to correct the systematic bias involved in the RCM simulations (e.g., Raty et al. 2014; Sarr et al. 2015; Sunyer et al. 2015). Although we do not ignore the potential for the uncorrected RCMs to induce a non-trivial effect in interpreting the climate change projection (Raty et al. 2014), we do not apply statistical bias correction to the four individual models participating in the ensemble in this study. The systematic biases in the underlying model can be partly canceled when taking the difference between the REF simulation and the RCP future projection, even though such a model bias could affect the magnitude of changes in response to emission forcing (Im et al. 2008; Hagemann and Jacob 2007; Sushama et al. 2006).

In this study, we investigate the changes in precipitation characteristics and hydroclimatic regimes in response to the RCP4.5 and RCP8.5 emission scenarios over the Korean peninsula and the surrounding region based on the multi-RCM projections that are combined with equal weighting from four different RCMs. The two RCP scenarios, namely RCP4.5, which is a stabilization scenario after about 2060 without overshooting pathways to 4.5 Wm<sup>-2</sup>, and RCP8.5, which is a rising pathway leading to 8.5 Wm<sup>-2</sup> by 2100, are used. These two scenarios are selected because they are the highest priority emission scenarios for global modeling studies under

the framework of the Coupled Model Intercomparison Project Phase 5 (CMIP5, Taylor et al. 2012), and consequently CORDEX (Giorgi et al. 2009). Inter-model comparison makes it possible to assess the uncertainty induced by RCM configurations, while the comparison between the RCP4.5 and RCP8.5 scenarios is meaningful for addressing the potential impact of mitigating GHG emissions. In particular, we focus on the hydroclimatic intensity index (HY-INT), which integrates the metrics of normalized precipitation intensity and normalized dry spell length because the response of these two metrics to global warming is deeply interconnected (Giorgi et al. 2011, 2014). HY-INT is a measure of changes in hydroclimatic regimes, with increasing HY-INT implying a shift toward a regime of more intense and less frequent precipitation events. Since HY-INT seems to be an indicator of overall hydroclimatic intensity rather than flood or drought extremes, we also examine two additional extreme indices: a dry extreme index, defined as the maximum number of consecutive dry days (CDD), and a wet extreme index, defined as the precipitation intensity above the 95 percentile (R95). We attempt to identify robust behaviors in both the mean precipitation and dry and wet extremes in response to enhanced emission scenarios and examine how these changes reflect hydroclimatic regimes.

To the best of our knowledge, only a few studies have examined the detailed characteristics of hydroclimatic change focusing on the Korean peninsula from the multi-RCM ensemble projections based on long-term (1981–2100), high-resolution (12.5 km), and daily time-scale output. In this regard, the updated assessment presented in this study can provide an opportunity to build on previous findings that assessed similar topics (e.g., Im et al. 2012a, b, 2015; Lee et al. 2013), thereby contributing to the firm ground of model-based projections of hydroclimatic changes over the Korean peninsula and the surrounding regions.

## 2 Experimental design and analysis method

### 2.1 RCM experimental design

In order to produce the customized climate information over the Korean peninsula and the surrounding region, dynamical downscaling is performed using four state-of-the-art RCMs, namely, GRIMs, HadGEM3-RA, RegCM4, and WRF, under the coordinated experimental design. Configurations common to all the four RCMs are the model domain setting and initial and boundary conditions. The domain covers the eastern regions of Asia centered at South Korea (37.5° N and 127.5° E), with 12.5-km horizontal resolution. The initial and lateral boundary conditions for running the four RCMs are taken from two global projections forced by different emission scenarios such as RCP4.5, a mid-level pathway, and RCP8.5, a

high-level one, using the Hadley Centre Global Environmental Model version 2–Atmosphere and Ocean (HadGEM2-AO, Collins et al. 2011). HadGEM2-AO has a horizontal resolution of  $1.875^\circ \times 1.25^\circ$ , and Baek et al. (2013) demonstrated that it showed reasonable performance over our target region (e.g., East Asia). Physical parameterizations and specifications used for the four individual RCMs are presented in Table 1. In terms of model dynamics, two RCMs (RegCM4 and GRIMs) are based on hydrostatic dynamical core while the others (HadGEM3-RA and WRF) are non-hydrostatic models. They all apply different physics parameterizations, which lead to considerable differences among their results (e.g., Bachner et al. 2008). Therefore, the spread among the RCMs can be interpreted as the uncertainty introduced by structurally different RCMs. Further detailed model descriptions can be also found in the references listed in Table 1.

## 2.2 Analysis method

To estimate the changes in hydroclimatic regimes, we calculate the hydroclimatic intensity index, HY-INT, which is defined as the combination of mean annual precipitation intensity (INT) and mean annual dry spell length (DSL) normalized by their climatological mean value, using daily precipitation (Giorgi et al. 2011, 2014). The value of HY-INT for a given year and location is simply given by

$$HY-INT = INT \times DSL.$$

Therefore, an increase in HY-INT can represent either an increase in both INT and DSL or an increase in one overwhelming a decrease in the other. In other words, HY-INT measures a dominant increase of INT, DSL, or both, and thus registers a change in the characteristics of the hydrologic cycle. Although HY-INT is an appropriate measure to indicate the overall pattern of hydroclimatic intensity, it is not intended to describe the wet or dry extremes such as drought and flood. To overcome this point, the analysis of two extreme indices is added. We select two extreme indices, namely, R95 and CDD,

to measure the extreme precipitation intensity and drought occurrence likelihood, which are recommended by the World Meteorological Organization Climate Variability and Predictability/JCOMM Expert Team on Climate Change Detection and Indices (Zhang et al. 2011). While R95 denotes the precipitation intensity exceeding the climatological 95th percentile precipitation, CDD indicates the maximum number of consecutive dry days, where a dry day is defined as having precipitation of less than 1 mm/day.

A two-tailed Student's *t* test is performed for the statistical significance of future changes for the late twenty-first century against present climate (2071–2100 relative to 1981–2010), while the statistical significance of trends in the indices is detected using the Mann–Kendall test, a widely used nonparametric test. In addition to the statistical significance test, we also assess the consistency among the four RCMs. It can directly support the robustness or agreement between projections simulated by the different RCMs.

## 3 Results

Since this study mainly investigates the robust response that appears in the projected regional climate, we do not focus on the validation of the accuracy of the four individual RCM's simulations of the present climate against observations. Instead, we only present one representative result that can demonstrate the reasonable performance of RCMs ensemble (hereafter referred to as ENS) as well as the advantage of dynamical downscaling over GCM in simulating the precipitation climatology. Figure 1 presents the spatial distribution of annual mean precipitation and its standard deviation derived from HadGEM2-AO driving GCM and ENS for the reference period (1981–2010). As for the observational pattern, the same quantities are also calculated using the Global Precipitation Climatology Project (GPCP) with monthly time-scale at  $2.5 \times 2.5$  horizontal resolution during the same period of reference simulation (Adler et al. 2003). First, mean precipitation shows a northwest gradient pattern of gradually

**Table 1** List of regional climate models (RCMs) used in this study and their configurations and details

	GRIMs	HadGEM3-RA	RegCM4	WRF
Dynamic framework	Hydrostatic	Non-hydrostatic	Hydrostatic	Non-hydrostatic
Vertical coordinate/levels	Sigma/28	Hybrid/38	Sigma/23	Eta/28
Convection scheme	SAS + CMT	Revised mass flux scheme	MIT-Emanuel	Kain-Fritsch II
Land surface	OML climatology value	MOSES-II	CLM3.5	Noah
LWR scheme	GSFC	Generalized 2-stream	CCM3	CAM
SWR scheme	GSFC	Generalized 2-stream	CCM3	CAM
Spectral nudging	Yes	No	Yes	No
References	Hong et al. (2013)	Davies et al. (2005)	Giorgi et al. (2012)	Skamarock et al. (2008)

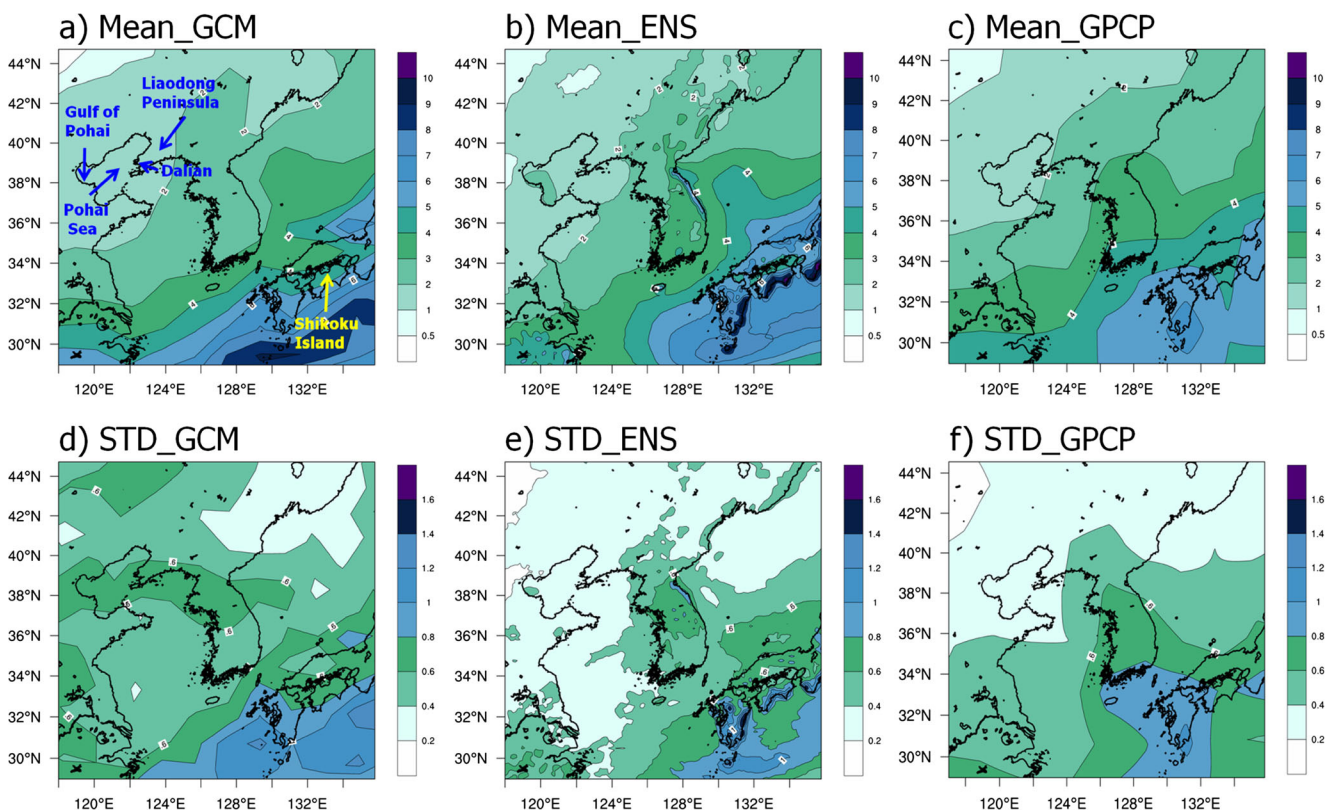


**Fig. 1** Spatial distribution of annual mean precipitation (a–c) and its standard deviation (d–f) derived from HadGEM2-AO (a, d) and ENS (b, e) reference simulation (1981–2010) and GPCP observation (c, f)

during the same period of simulation. **a** includes the name of places where a relevant signal appeared in the changes in the characteristics of future precipitation

decreasing amount from the southern region of Kyushu and Shikoku Island. By comparison with GCM, ENS shows better agreement with the GPCP observational pattern in reproducing spatial variations. While GPCP shows a regionally high value ranging between 3 and 4 mm/day centered on the Korean peninsula, GCM produces a shape that protrudes completely over East Sea of the Korean peninsula. ENS also shows a slightly easterly shifted pattern, but mean precipitation covering between 3 and 4 mm/day appears in the southern part of the Korean peninsula, similar to GPCP. The improvement by ENS is also found in the spatial pattern of variability measured by standard deviation. The ENS pattern is more correlated with GPCP than with GCM. The ratio of the standard deviation to the mean (not shown) infers a high degree of variation over the middle and southern parts of the Korean peninsula. More detailed validation of the four models used in this study can be found in many previous studies (i.e., Park et al. 2015; Oh et al. 2014; Im et al. 2015; Hong and Ahn 2015; Lee and Hong 2014; Seo et al. 2015). They demonstrated that RCMs overall show a reasonable performance in capturing key features of the regional climate associated with the East Asian monsoon, in spite of some systematic biases.

Now, we examine the future change of ENS by investigating the difference between reference simulation and RCP future projection. Figure 2 presents the spatial distributions of

30-year climatological changes (2071–2100 relative to 1981–2010) in annual mean precipitation derived from HadGEM2-AO driving GCM and ENS forced by the RCP4.5 and RCP8.5 emission scenarios. For brevity, the spatial distributions of RCM results are only presented by ENS instead of the four individual RCMs. In general, ENS shows similar change patterns to those of HadGEM2-AO, except for spatial details that are mostly smoothed out or eliminated in the coarse-grid GCM simulations. Most of the domains in the RCP4.5 scenario are dominated by large increases in precipitation, in spite of some limited areas with precipitation decrease. As the emission forcing is enhanced (i.e., RCP8.5), the magnitude of the precipitation increase becomes much stronger and the entire domain experiences increased precipitation, except for the southern region of Kyushu and Shikoku Island (i.e., the southeastern boundary of the domain). In addition, the RCP8.5 projection further extends the areas where the changes are statistically significant at the 95 % confidence level, whereas the statistical significance of changes seen in the RCP4.5 projection is mostly restricted to the southern part of the domain, mainly passing through the East China Sea. Therefore, stronger emission forcing is capable of producing a more amplified and significant response, which is in line with many other studies that compared future climate behaviors under the RCP4.5 and RCP8.5 scenarios (i.e., Im et al. 2015).

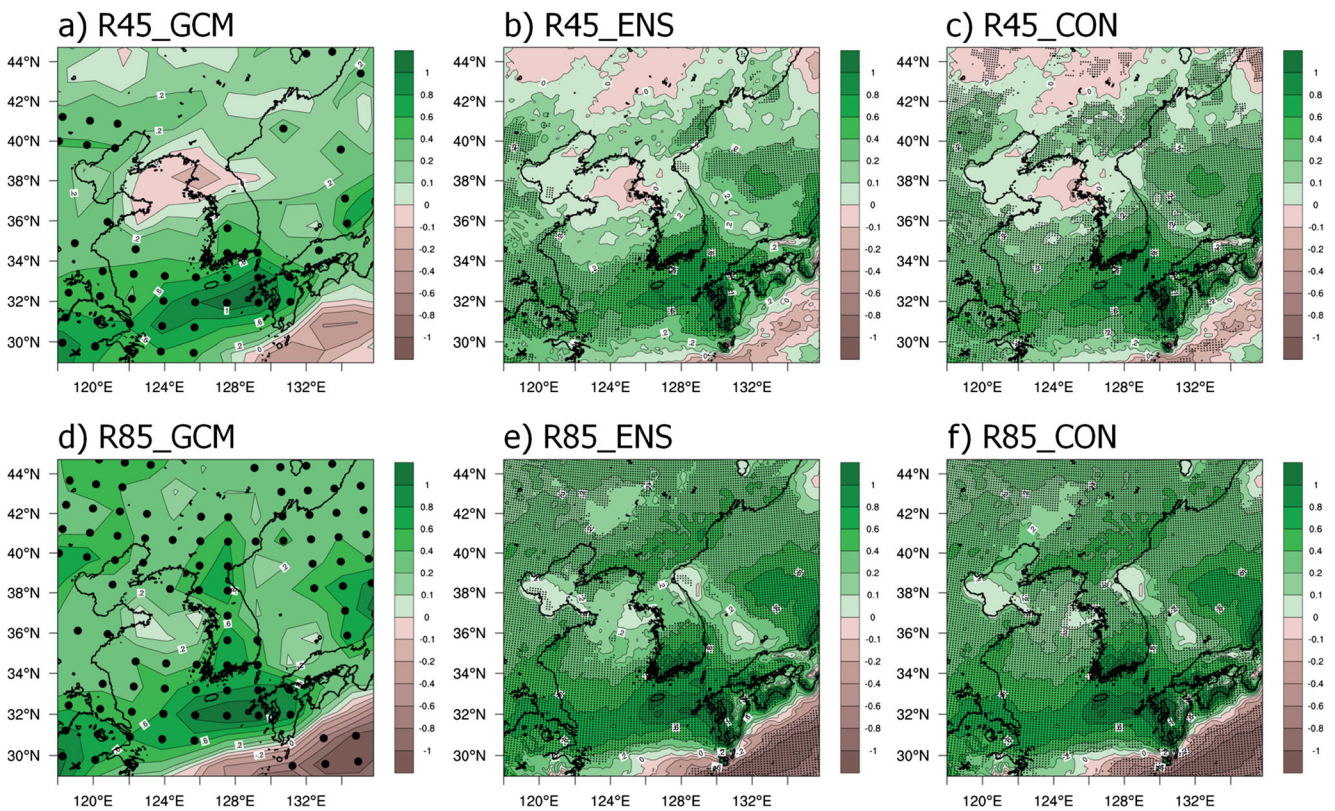


**Fig. 2** Spatial distribution of changes (2071–2100 relative to 1981–2010) in annual mean precipitation (mm/day) derived from HadGEM2-AO (**a**, **d**) and ENS (**b–c**, **e–f**) in response to the RCP4.5 (**a–c**) and RCP8.5 (**d–f**) scenarios; **b** and **e** have the same shading with **c** and **f**, but with different *superimposed dots*. While **b** and **e** *superimpose dots* in

the areas where the changes are statistically significant at the 95 % confidence level based on the Student's *t* test, *superimposed dots* in **c** and **f** indicate 100 % of inter-model agreement (four RCMs agrees with the sign of changes)

Interestingly, the regions where the four RCMs all agree with the sign of changes in precipitation become more widespread, compared to the regions that are satisfied with the conventional statistical test (i.e., Student's *t* test). This implies that although the forced signal in response to the RCP scenarios seems too small to overwhelm the internal variability (i.e., interannual and interdecadal variability), the RCMs exhibit a common response engineered toward the same direction of change due to enhanced GHGs forcing. This insensitivity to the different RCMs provides some confidence for the impact of GHGs on precipitation.

To prevent erroneous interpretation of the results from a certain period, we examine the long-term trend of precipitation covering an 80-year future period (i.e., 2021–2100). Indeed, the change pattern of 30-year average precipitation (2071–2100) seen in Fig. 2 does not guarantee consistent tendencies in the temporal evolution across the whole twenty-first century, due to the large variability of local- to regional-scale precipitation (i.e., Im et al. 2008). Figure 3 presents the spatial distribution of the linear trend in mean precipitation during 2021–2100. Three relevant features appear to be similar to the behavior of the 30-year mean precipitation. First, the upward trend is dominant, except for some limited regions.

Second, the changes in the RCP8.5 are stronger and more significant than those in the RCP4.5. Lastly, the robust feature exhibits a greater extent in model agreement than in the statistical significance test. On the other hand, the geographical patterns of changed magnitudes between 30-year climatological mean precipitation (2071–2100) and 80-year long-term trend (2021–2100) are somewhat different. For example, the South China Sea and southern coastal area of the Korean peninsula exhibit a strong intensification in mean precipitation for the late twenty-first century (i.e., 2071–2100), although the long-term trends over that region show a relatively gentle upward trend. Rather, a pronounced upward trend manifests in the northern part of the Korean peninsula in the RCP8.5 projection. In addition, it is worth addressing the opposite sign between the 80-year trend and the 30-year mean change appearing in the RCP4.5 projection. For example, when looking into the Korea Bay separated from the Pohai Sea by the Liaodong Peninsula with Dalian at its southernmost point and looking into the southern region of Shikoku Island, which witnesses decreased precipitation in 2071–2100 (Fig. 2b, c), slightly increasing trends are evident despite not being statistically significant due to higher variability than the upward trend. This discrepancy over both regions is attributed to the

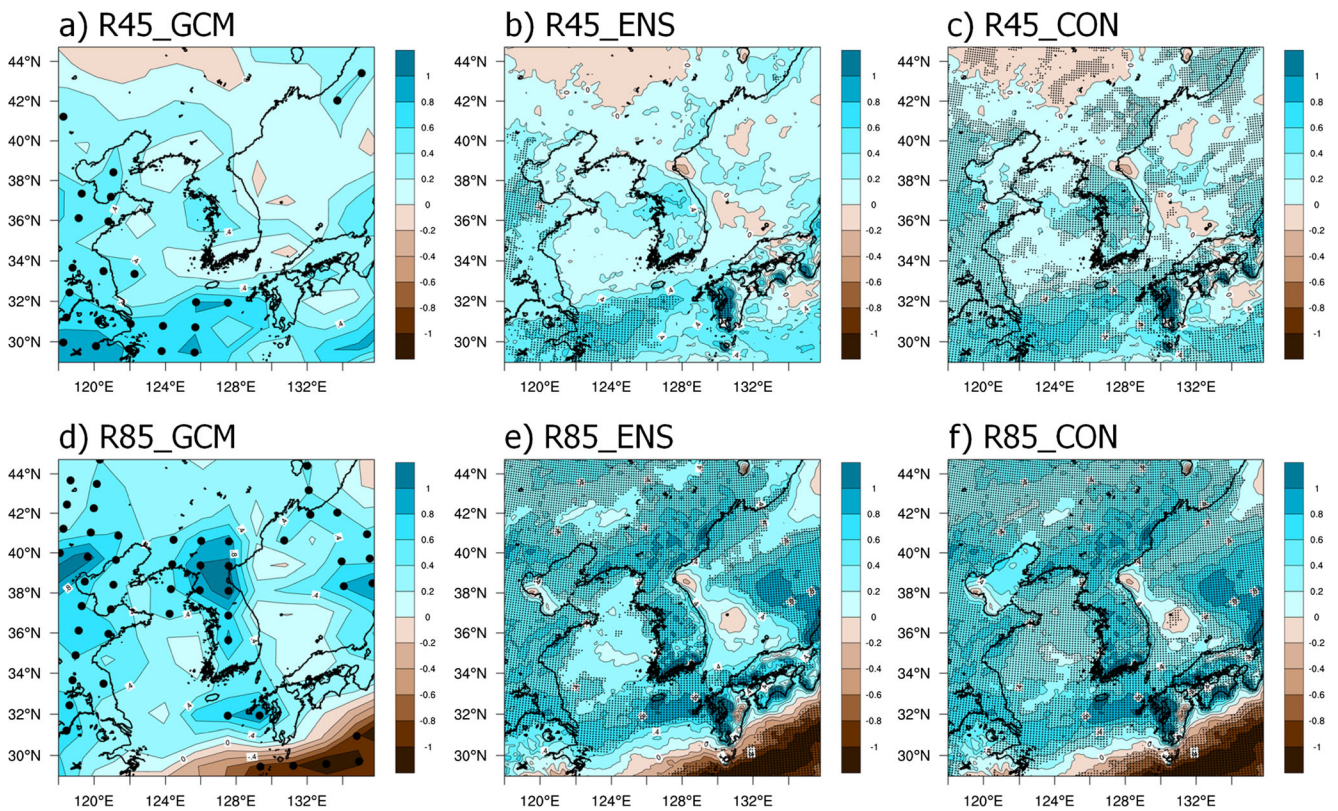


**Fig. 3** Same as in Fig. 2 but for long-term trend (2021–2100) of annual mean precipitation (mm/day); **b** and **e** superimpose dots in the areas where the trend is statistically significant at the 95 % confidence level based on a nonparametric Mann–Kendall test

sudden drop of mean precipitation in the 2090s (not shown). This can lead to decreased precipitation over a certain period, but cannot change the general direction of the long-term trend.

Keeping in mind the changes in mean precipitation, we move our attention to the change of HY-INT. Figure 4 presents the spatial distribution of changes in normalized INT, DSL, and HY-INT. The spatial patterns of INT change are generally correlated with those of mean precipitation, but their statistical significance becomes stronger across the broader region. In particular, stronger enhancement of INT along the Gulf of Pohai and the northern Korean peninsula is relevant in the RCP8.5 projection, rather than the southern part of the domain, where an increase in mean precipitation is dominant; this is a tribute to the northward movement of the Changma-related stationary front (Hong and Ahn 2015). Hong and Ahn (2015) demonstrated that the intensity of heavy precipitation during the Changma period increases dominantly in the Gulf of Pohai, particularly under the RCP8.5 scenario, from the WRF-downscaled projection used as one member of ENS in this study. The change in DSL shows different behavior with INT in terms of spatial variation and statistical significance. However, the changes in INT and DSL both show a relevant increase over the Gulf of Pohai, which induces much stronger HY-INT over that region. Both the Gulf of Pohai and the whole domain (except for a small area in the northwestern corner) exhibit a strong increase in HY-INT for the late twenty-first

century. In addition, in most of the regions, this increase is statistically significant at the 95 % confidence level (superimposed dots in Fig. 4c, f), and almost all regions are satisfied by the model agreement (not shown). In general, HY-INT induces more robust response to enhanced GHGs emissions (i.e., RCP4.5 and RCP8.5 scenarios), compared to the changes in mean precipitation. Based on our projection, there are large increases of HY-INT over the Gulf of Pohai and the northern part of the Korean peninsula, implying increased risks and vulnerability to hydroclimatic stress. This demonstrates that the increase or decrease of mean precipitation provides only limited information in terms of hydroclimatic stress. For example, extreme precipitation can be significantly enhanced without the increasing mean precipitation (Im et al. 2012b), whereas the increase of mean precipitation due to the contribution of heavy precipitation is not very helpful for reducing the drought condition. This demonstrates the necessity of understanding the changes in precipitation characteristics (Trenberth et al. 2003). In this regard, HY-INT is a good indicator to measure future changes in hydroclimatic stress.

The long-term trend of HY-INT is also investigated. Figure 5 presents the spatial distribution of the linear trend of the temporal evolution in HY-INT from 2021 to 2100. An upward trend is dominant across the whole domain except for a few small locations. Compared to the 30-year changes in HY-INT, the statistical significance using the Mann–Kendall test is

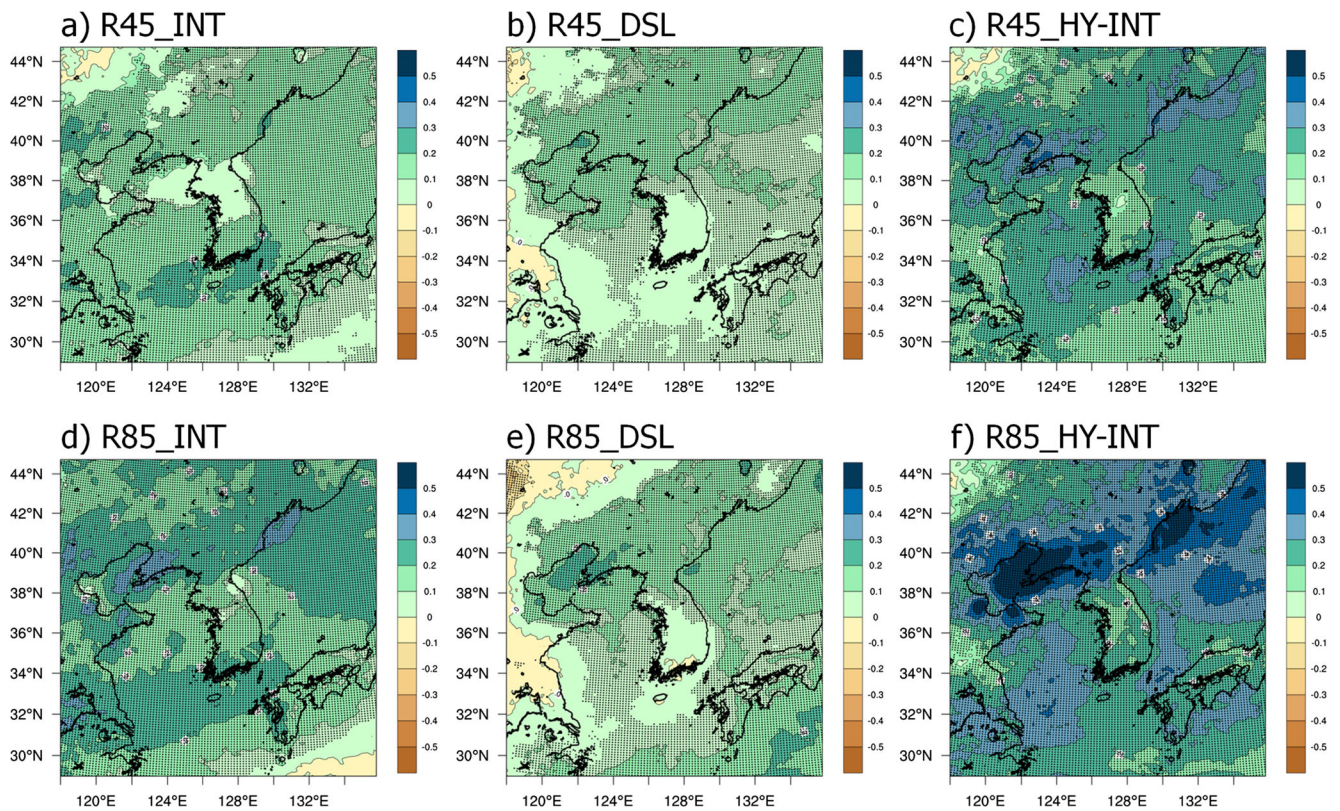
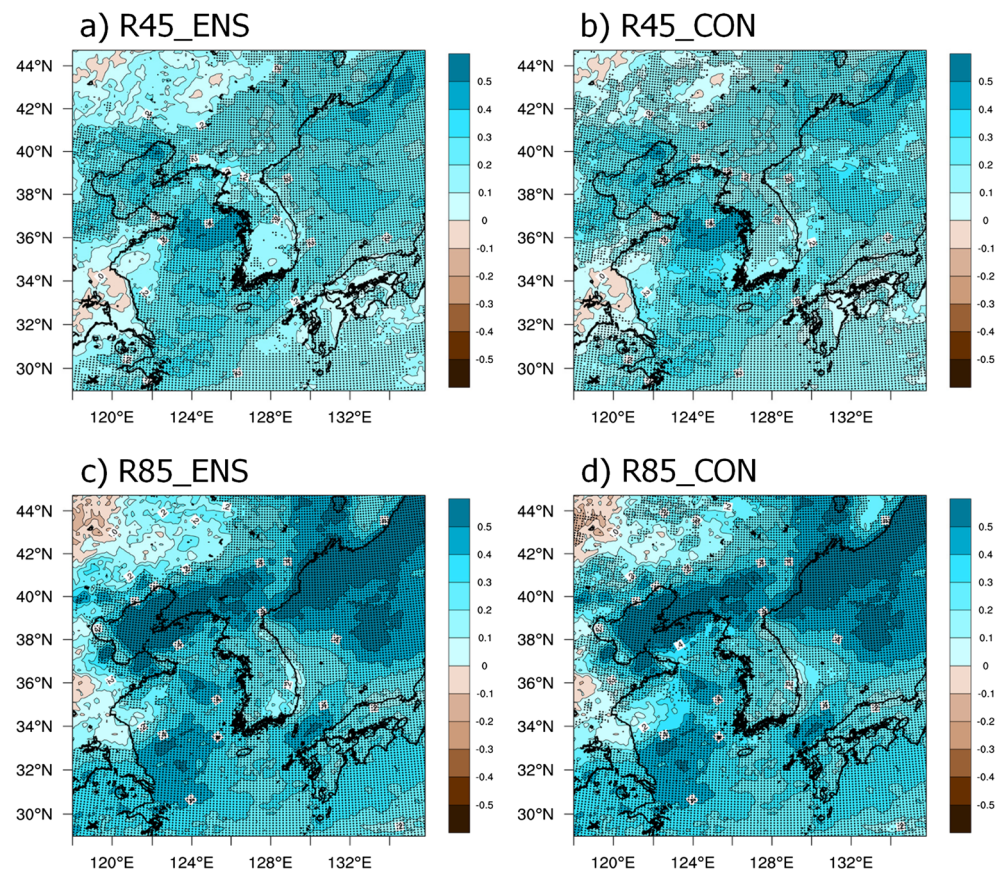


**Fig. 4** Spatial distribution of changes (2071–2100 relative to 1981–2010) in INT, DSL, and HY-INT derived from ENS in response to the RCP4.5 (a–c) and RCP8.5 (d–f) scenarios. *Superimposed dots* indicate statistical significance at the 95 % confidence level based on the Student's *t* test

**Fig. 5** Spatial distribution of long-term trend (2021–2100) of HY-INT from ENS in response to the RCP4.5 (a, b) and RCP8.5 (c, d) scenarios. While a and c *superimpose dots* in the areas where the trend is statistically significant at the 95 % confidence level based on a nonparametric Mann–Kendall test, *superimposed dots* in b and d indicate 100 % of inter-model agreement (four RCMs agrees with the sign of changes)



limited over the Korean peninsula, particularly in the RCP4.5 projection. Therefore, it is assumed that the upward trend induced by the RCP4.5 scenario is not strong enough to overwhelm the natural variability over the Korean peninsula. In general, HY-INT exhibits robust changes in not only 30-year climatology but also 80-year trends, compared to the changes in mean precipitation.

Even though HY-INT includes the occurrence of extremes such as drought and floods, it can also reflect the changes in light events, which makes it appropriate to measure overall hydroclimatic intensity rather than focusing on extremes (Giorgi et al. 2011). Therefore, we also examine the changes in two extreme indices to accurately represent the wet and dry extremes. R95 and CDD are indicators of the magnitude of wet extreme and of the persistence of dry extreme, respectively. Figures 6 and 7 present the spatial distribution of changes in R95 and CDD derived from the RCP4.5 and RCP8.5 projections. The magnitude of changes in R95 is much stronger than that from mean precipitation (Fig. 2) and daily mean intensity (Fig. 4). R95 exhibits significant increases across almost the entire domain. The spatial coherence between R95 and INT is high, but the intensification of R95 is further extended. Furthermore, the majority of changes in R95 is statistically significant at the 95 % confidence level, which is an improved feature compared to changes in mean precipitation

and mean intensity change. In contrast to the changes in R95, projected CDD for the late twenty-first century shows a mixed signal with both increasing and decreasing changes, and its statistical significance is quite limited. Therefore, it is difficult to interpret the result as robustly as the R95 derivation. Nevertheless, large areas in the domain exhibit a CDD increase in common across all the four RCMs. A CDD increase is projected across roughly the northern half of the domain for all the four RCMs under both the RCP4.5 and RCP8.5 scenarios. Interestingly, the impact of enhanced GHGs emission (i.e., RCP4.5 vs. RCP8.5) is relatively small compared to R95. While R95 tends to be sensitive to emission forcing, showing much stronger increase in the RCP8.5 projection, CDD shows a somewhat limited response to emission forcing in terms of the intensification of CDD and improvement of the statistical significance. The spatial pattern shows a general agreement with DSL (Fig. 4); however, the magnitude of change around the Gulf of Pohai becomes far stronger. Comparing CDD and R95 with mean precipitation, it appears that the increase in dry and wet extremes is not specifically tied to the precipitation change, which is in line with Giorgi et al. (2014). This is spatially the case for the Gulf of Pohai. The ENS produced in this study suggests that the Gulf of Pohai is prone to suffer both wet and dry extremes, which will increase its vulnerability to water management under global warming.

**Fig. 6** Spatial distribution of changes (2071–2100 relative to 1981–2010) in heavy precipitation index (R95: mm/day) derived from ENS in response to the RCP4.5 (a, b) and RCP8.5 (c, d) scenarios. While a and c superimpose dots in the areas where the changes are statistically significant at the 95 % confidence level based on the Student's *t* test, superimposed dots in b and d indicate 100 % of inter-model agreement (four RCMs agrees with the sign of changes)

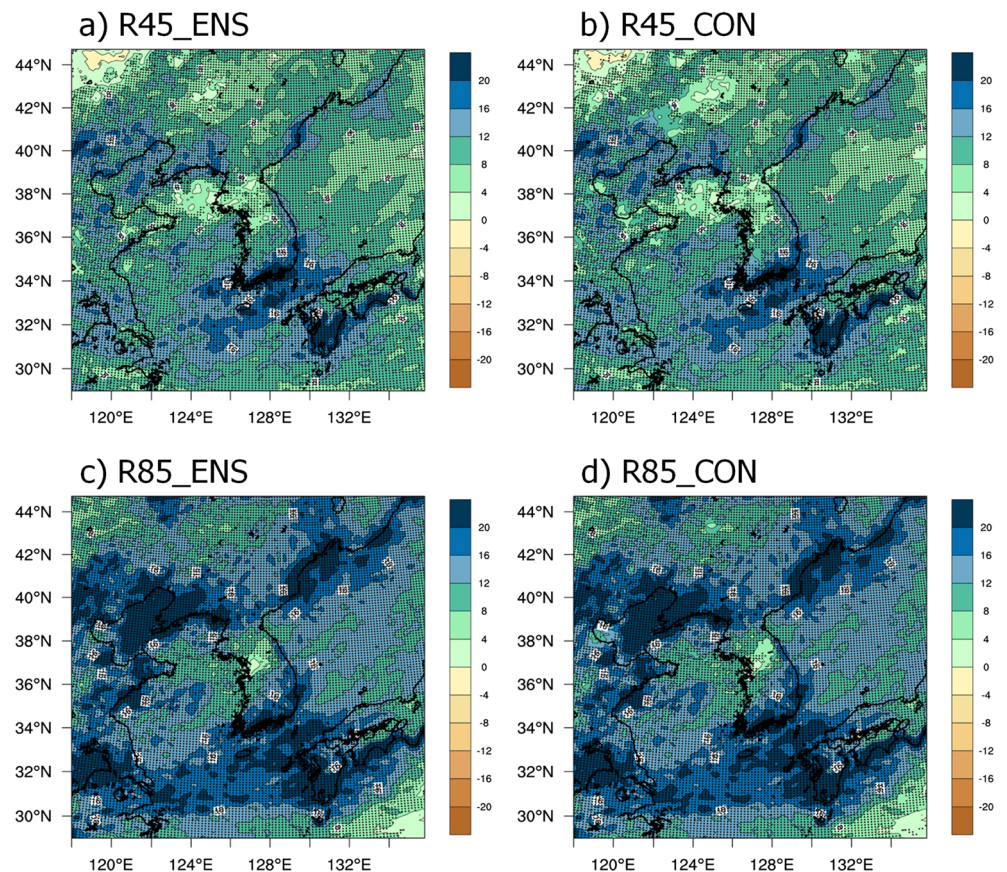
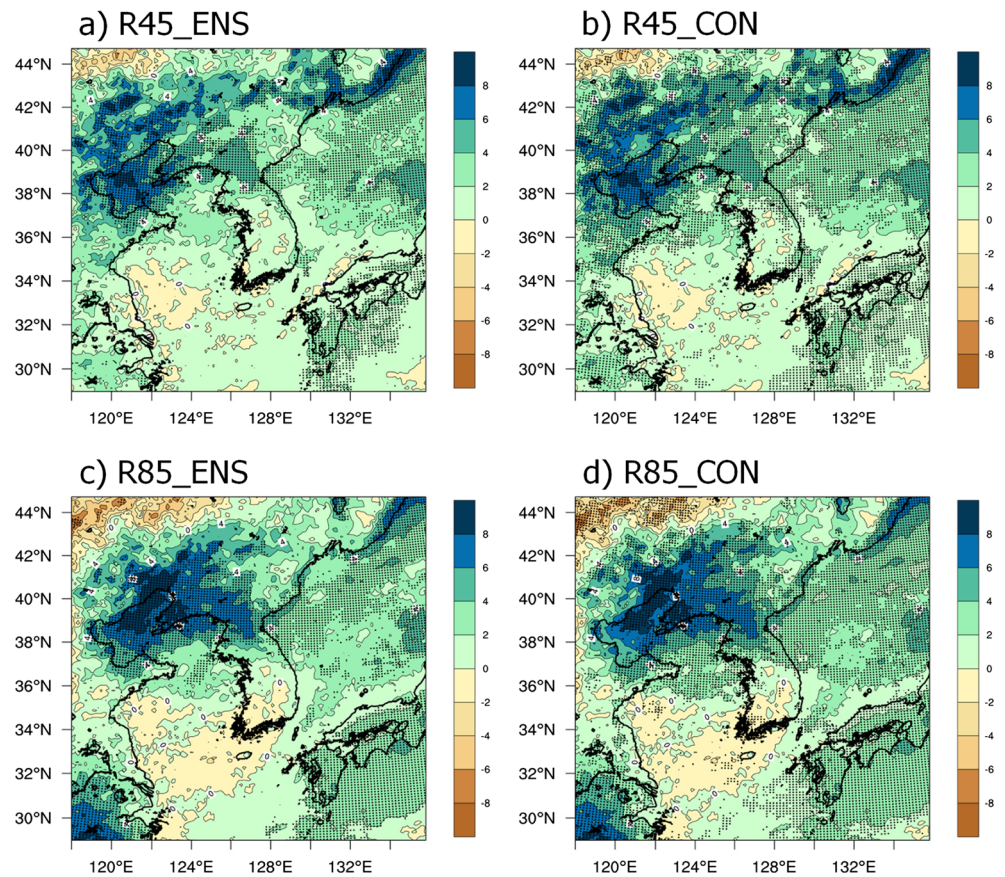


**Fig. 7** Same as in Fig. 6 but for maximum number of consecutive dry days (CDD: days)



Figures 4, 5, 6, and 7 reveal that the enhanced GHGs emission could increase the hydroclimatic intensity, thereby producing the robust response of increasing both wet and dry extremes over East Asia centered on the Korean peninsula beyond the increase in mean precipitation. As indicated by HY-INT and the two extreme indices, the crux is the changes in precipitation characteristics rather than the changes in mean precipitation. For example, increasing mean precipitation does not necessarily decrease the possibility of dry extremes like CDD in this study (e.g., Liaoning peninsula). To quantitatively examine the changed characteristics of daily precipitation, we display the precipitation change for the late twenty-first century (2071–2100) across various intensity ranges (Fig. 8). In addition to the whole domain of East Asia, we also perform the same analysis over two sub-regions (i.e., the Gulf of Pohai: lat = 38–42 N and lon = 119–124 E and South Korea: lat = 34–38 N and lon = 125–130 E), where HY-INT shows different behavior. This analysis reveals the relative contribution of low and high intensity precipitation to the change of total amount under the warming scenario. The most consistent pattern appearing in all cases is an enhancement of relatively high intensity precipitation and a reduction of weak intensity precipitation. In general, the contrast rates of increasing and decreasing tend to be enhanced as GHGs emission forcing becomes stronger (i.e., RCP8.5). Comparing the Gulf of Pohai

and South Korea, the change patterns over these sub-regions show general agreement in terms of the change direction, but their magnitude is somewhat different. The change distribution over the Gulf of Pohai shows a sharp gradient in accordance with intensity. The decrease in a large amount of weak precipitation supports the increase of CDD, while the increase in relatively high intensity precipitation makes favorable condition for the enhancement of R95. Therefore, despite the absence of any significant changes in mean precipitation, the Gulf of Pohai is capable of producing a higher HY-INT.

To comprehensively examine the hydrological sensitivity in response to increased temperature, we calculate the changes in mean precipitation, HY-INT, CDD, and R95 from the four individual RCMs projections and their ensemble as a function of temperature for eight successive decadal periods (2021–2100) (Fig. 9). Since temperature increase is roughly proportional to the GHG emissions (Im et al. 2015), the RCP8.5 projections offer much wider ranges of decadal-averaged temperature than those from the RCP4.5 projections. By comparison with linear regression lines fitted to the four individual RCMs projections and their ensemble, the HY-INT increase rate is predominant, clearly indicating its large sensitivity to temperature. For example, ENS under the RCP8.5 scenario produces approximately 39 and 16 % increases of HY-INT and mean precipitation during the last decade of the twenty-

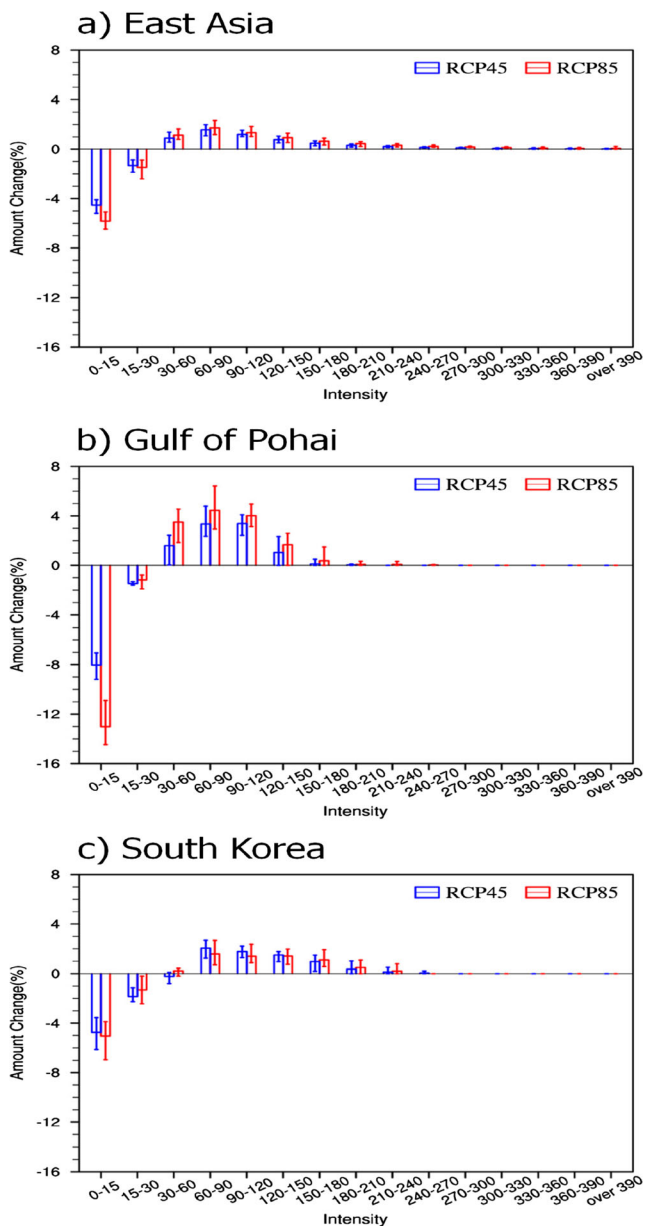


**Fig. 8** Changes (2071–2100 relative to 1981–2010) in amount of daily precipitation accumulated over all the precipitation events contributing for each intensity bin over East Asia (a), the Gulf of Pohai (b), and South Korea (c). Histogram bins outlined in blue and red are respectively derived from ENS in response to the RCP4.5 and RCP8.5 scenarios, and the vertical error bar in the middle of each bin indicates the inter-model spread measured by the four individual RCM projections

first century (2091–2100), respectively. Given a temperature increase of 5.1 °C for the last decadal period of twenty-first century from ENS under the RCP8.5 (2091–2100 relative to 1981–2010), the sensitivities of HY-INT and mean precipitation to temperature are about 7.6 and 3.1 % per degree of warming, respectively. The temperature sensitivity of HY-INT (7.6 %) is more than twice that of mean precipitation (3.1 %), and the value of 7.6 % roughly agrees with that theoretically estimated from the C–C relationship. This is

consistent with findings from Giorgi et al. (2011). Kusunoki and Mizuta (2013) also demonstrated that the response of mean precipitation to temperature increase is less effective than precipitation intensity or extremes. Interestingly, the coefficient of the slope of the HY-INT regression line is larger in the RCP4.5 projection (8.0 %/K) than in the RCP8.5 projection (7.1 %/K), indicating a steeper gradient of the RCP4.5 projection. Although the absolute increase rate of HY-INT is higher in the RCP8.5 projection than that in the RCP4.5 projection, the larger increment of temperature from the RCP8.5 projection could weaken the response to the warming degree. While the gradient of the regression line supports the efficiency of the corresponding quantity per degree of warming, the standard errors of the regression coefficient can measure the precision of the estimate of the coefficient. In this respect, the RCP8.5 projection shows greater precision with smaller standard errors of the regression coefficient (i.e., 0.84 for the RCP8.5 vs. 1.69 for the RCP4.5). Indeed, the dispersion is evidently more spread in the RCP4.5 projection than that in the RCP8.5 projection. Nevertheless, more importantly, the RCP4.5 emission scenario and the corresponding temperature increase are probably large enough to induce significant changes in hydroclimatic intensity, despite the limited statistical precision.

#### 4 Summary and discussion

In this study, we analyze the multi-RCM ensemble projections that have been newly generated for fine-scale (12.5 km) reliable climate information over East Asia centered on the Korean peninsula. The four different RCMs, namely, WRF, HadGEM3-RA, RegCM4, and GRIMs, are used for dynamical downscaling of the HadGEM2-AO global projections forced by the RCP4.5 and RCP8.5 scenarios. We focus on the changes in hydroclimatic intensity under the different GHGs emission forcing (RCP4.5 vs. RCP8.5). Not only annual mean precipitation but also HY-INT, which integrates the metrics of normalized precipitation intensity and normalized dry spell length, are investigated in terms of 30-year climatological change for the late twenty-first century (2071–2100) and long-term trend (2021–2100). The changes in dry and wet extremes are also estimated based on the maximum number of consecutive dry days (CDD) and heavy precipitation index defined as precipitation intensity above the 95 percentile (R95), respectively.

Annual mean precipitation is likely to increase in the majority of the domain. While the change in mean precipitation is tied to the regional change in precipitation intensity, the increase in mean precipitation does not necessarily mean less dryness measured in terms of dry spell length. It brings the inconsistency in geographical pattern between mean precipitation and HY-INT. HY-INT shows a predominant increase in

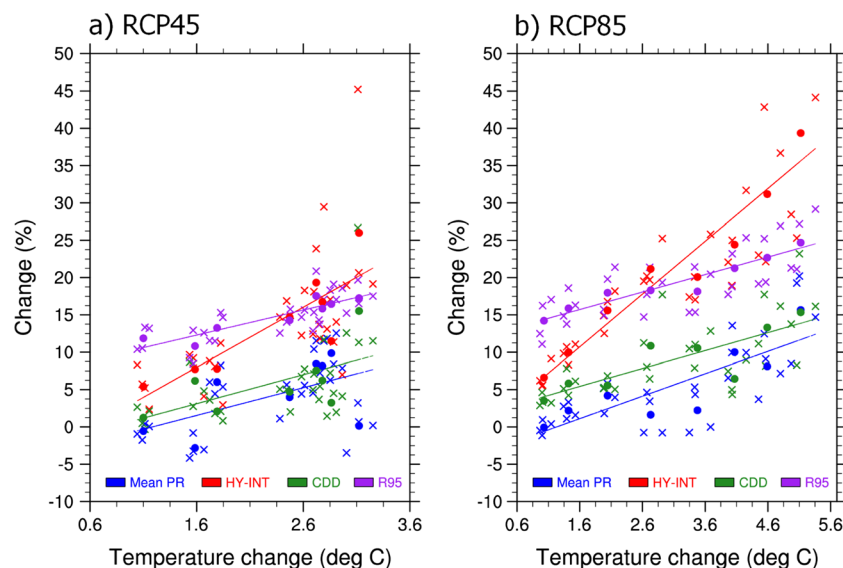


**Fig. 9** Changes in mean precipitation, HY-INT, CDD, and R95 as a function of temperature increase for eight successive decadal periods (2021–2030 up to 2091–2100). The multiplication sign ( $\times$ ) indicates the change of each variable derived from the four individual RCMs, and the

closed circle denotes their ensemble with respect to the corresponding decade and variable. Linear regression lines are fitted to the four individual RCMs projection and their ensemble

response to the RCP4.5 and RCP8.5 emission forcings, with greatest intensification over the Gulf of Pohai and the northern part of the Korean peninsula. In particular, significant increases in both CDD and R95 emerge over the Gulf of Pohai, where the response of mean precipitation is relatively less intense than in other regions (e.g., the southern coastal region of the Korean peninsula). It can be an example to demonstrate that the increase or decrease in dry and wet extremes is not distinctly tied to the precipitation change, but rather reflects a possible shift in hydroclimatic regime, which is in line with Giorgi et al. (2014). Indeed, our projections clearly suggest that enhanced GHGs emission forcings can affect the precipitation characteristics through systematic redistribution of the intensity and frequency of daily precipitation. All the projections consistently show an enhancement of high intensity precipitation and a reduction of weak intensity precipitation, which in turn induces a possible shift in hydroclimatic regime prone to an increase of both wet and dry extremes. This finding may have important implications for water resources management. In other words, the changes in total precipitation averaged over a relatively long period are often insufficient to adequately provide valuable information to cope with multifaceted matters caused by the changing characteristics of precipitation.

The direction of the changes in precipitation characteristics appears to be a consistent and robust signature in response to enhanced GHGs emission forcing. Our study findings support those of similar previous studies, and thus enhance the robustness of increasing hydroclimatic intensity under global

warming. Considering that the RCM projection is dependent on driving GCM, future research should examine the ensemble projections of combined multi-RCMs and multi-GCMs.

**Acknowledgment** This work was funded by the Korea Meteorological Administration Research and Development Program under grant KMIPA 2015–2081 and the Rural Development Administration Cooperative Research Program for Agriculture Science and Technology Development under Grant Project No. PJ012293, Republic of Korea.

**Open Access** This article is distributed under the terms of the Creative Commons Attribution 4.0 International License (<http://creativecommons.org/licenses/by/4.0/>), which permits unrestricted use, distribution, and reproduction in any medium, provided you give appropriate credit to the original author(s) and the source, provide a link to the Creative Commons license, and indicate if changes were made.

## References

- Adler RF, Huffman GJ, Chang A, Ferraro R, Xie PP, Janowiak J, Rudolf B, Schneider U, Curtis S, Bolvin D, Gruber A, Susskind J, Arkin P, Nelkin E (2003) The version 2 Global Precipitation Climatology Project (GPCP) monthly precipitation analysis (1979–present). *J Hydrometeorol* 4:1147–1167
- Allen MR, Ingram WJ (2002) Constraints on the future changes in climate and the hydrological cycle. *Nature* 419:224–232
- Bachner S, Kapala A, Simmer C (2008) Evaluation of daily precipitation characteristics in the CLM and their sensitivity to parameterizations. *Meteorol Z* 17:407–419
- Baek HJ, Lee J, Lee HS, Hyun YK, Cho C, Kwon WT, Marzin C, Gan SY, Kim MJ, Choi DH, Lee J, Lee J, Boo KO, Kang HS, Byun YH (2013) Climate change in the 21st century simulated by HadGEM2-

- AO under representative concentration pathways. *Asia-Pac J Atmos Sci* 49:603–618
- Chou C, Chen CA, Tan PH, Chen KT (2012) Mechanisms for global warming impacts on precipitation frequency and intensity. *J Clim* 25:3291–3306
- Collins WJ, Bellouin N, Doutriaux-Boucher M, Gedney N, Halloran P, Hinton T, Hughes J, Jones CD, Joshi M, Liddicoat S, Martin G, O'Connor F, Rae J, Senior C, Sitch S, Totterdell I, Wiltshire A, Woodward S (2011) Development and evaluation of an earth-system model—HadGEM2. *Geosci Model Dev* 4:997–1062. doi:10.5194/gmd-4-1051-2011
- Davies T, Cullen MJP, Malcolm AJ, Mawson MH, Staniforth A, White AA, Wood N (2005) A new dynamical core for the met office's global and regional modeling of the atmosphere. *QJR Meteorol Soc* 131:1759–1782. doi:10.1256/qj.04.101
- Deque M, Rowell DP, Luthi D, Giorgi F, Christensen JH, Rockel B, Jacob D, Kjellstrom E, de Castro M, van den Hurk B (2007) An intercomparison of regional climate simulations for Europe: assessing uncertainties in model projections. *Clim Chang* 81:53–70
- Endo H, Kitoh A (2014) Thermodynamic and dynamic effects on regional monsoon rainfall changes in a warmer climate. *Geophys Res Lett* 41:1704–1710
- Fischer EM, Sedlacek J, Hawkins E, Knutti R (2014) Models agree on forced response pattern of precipitation and temperature extremes. *Geophys Res Lett* 41:8554–8562. doi:10.1002/2014GL062018
- Freychet N, Hsu H-H, Chou C, Wu C-H (2015) Asian summer monsoon in CMIP5 projections: a link between the change in extreme precipitation and monsoon dynamics. *J Clim* 28:1477–1493
- Gao XJ, Yu Y, Zhao Z, Pal JS, Giorgi F (2006) On the role of resolution and topography in the simulation of East Asia precipitation. *Theor Appl Climatol* 86:173–185
- Gao XJ, Shi Y, Zhang D, Wu J, Giorgi F, Ji Z, Wang Y (2012) Uncertainties in monsoon precipitation projections over China: result from two high-resolution RCM simulations. *Clim Res* 52:213–226
- Giorgi F, Mearns LO (2003) Probability of regional climate change based on the reliability ensemble averaging (REA) method. *Geophys Res Lett* 30:31–31. doi:10.1029/2003GL017130
- Giorgi F, Jones C, Asrar GR (2009) Addressing climate information needs at the regional level: the CORDEX framework. *WMO Bull* 58:175–183
- Giorgi F, Im ES, Coppola E, Diffenbaugh NS, Gao XJ, Mariotti L, Shi Y (2011) Higher hydroclimatic intensity with global warming. *J Clim* 24:5309–5324
- Giorgi F, Coppola E, Solmon F, Mariotti L, Sylla MB, Bi X, Elguindi N, Diro GT, Nair V, Giuliani G, Cozzini S, Gu'tler I, TA O'B, AB T, Shalaby A, AS Z, AL S, Stordal F, LC S, Brankovic C (2012) RegCM4: model description and preliminary tests over multiple CORDEX domains. *Clim Res* 52:7–29
- Giorgi F, Coppola E, Raffaele F, Diro GT, Fuentes-Franco F, Giuliani G, Mamgain A, Llopart-Pereira M, Mariotti L, Torma C (2014) Changes in extremes and hydroclimatic regimes in the CREMA ensemble projections. *Clim Chang* 125:39–51
- Hagemann S, Jacob D (2007) Gradient in the climate change signal of European discharge predicted by a multi-model ensemble. *Clim Chang* 81:309–327
- Held IM, Soden BJ (2006) Robust response of the hydrological cycle to global warming. *J Clim* 19:5686–5699
- Hong J-Y, Ahn J-B (2015) Changes of early summer precipitation in the Korean peninsula and nearby regions based on RCP simulations. *J Clim* 28:3557–3578
- Hong S-Y, Park H, Cheong H-B, Kim J-EE, Koo M-S, Jang J, Ham S, Hwang S-O, Park B-K, Chang E-C, Li H (2013) The global/regional integrated model system (GRIMs). *Asia-Pac J Atmos Sci* 49:219–243
- Im E-S, Gutowski WJ, Giorgi F (2008) Consistent changes in twenty-first century daily precipitation from regional climate simulations for Korea using two convection parameterizations. *Geophys Res Lett* 35:L14706. doi:10.1029/2008GL034126
- Im E-S, Ahn J-B, Kim D-W (2012a) An assessment of future dryness over Korea under global warming from the RegCM3-ECHAM5 model chain under A1B emission scenario. *Asia-Pac J Atmos Sci* 48:325–337
- Im E-S, Lee BJ, Kwon JH, In SR, Han SO (2012b) Potential increase of flood hazards in Korea due to global warming from a high-resolution climate simulations. *Asia-Pac J Atmos Sci* 48:107–113
- Im E-S, Ahn J-B, Jo S-R (2015) Regional climate projection over South Korea simulated by the HadGEM2-AO and WRF model chain under the RCP emission scenarios. *Clim Res* 69:249–266
- IPCC (2013) Stocker TF, Qin D, Plattner GK, Tignor M and others (eds) *Climate change 2013: the physical science basis. Contribution of Working Group I to the Fifth Assessment Report of the Intergovernmental Panel on Climate Change*. Cambridge University Press, Cambridge.
- Kendon EJ, Rowell DP, Jones RG, Buonomo E (2008) Robustness of future changes in local precipitation extremes. *J Clim* 21:4280–4297
- Knutti R, Furrer R, Tebaldi C, Cernak J, Meehl GA (2010) Challenges in combining projections from multiple climate models. *J Clim* 23:2739–2758
- Kusunoki S, Mizuta R (2013) Changes in precipitation intensity over East Asia during the 20th and 21st centuries simulated by a global atmospheric model with a 60 km grid size. *J Geophys Res Atmos* 118:11007–11016
- Lau WK-M, Wu H-T, Kim K-M (2013) A canonical response of precipitation characteristics to global warming from CMIP5 models. *Geophys Res Lett* 40:3163–3169
- Lee JW, Hong SY, Chang EC, Suh MS, Kang HS (2013) Assessment of future climate change over East Asia due to the RCP scenarios downscaled by GRIMs-RMP. *Clim Dyn* 42:733–747
- Lee JW, Hong SY (2014) Potential for added value to downscaled climate extremes over Korea by increased resolution of a regional climate model. *Theor Appl Climatol* 117:667–677
- Min S-K, Hense A (2006) A Bayesian approach to climate model evaluation and multi-model averaging with an application to global mean surface temperature from IPCC AR4 coupled climate models. *Geophys Res Lett* 33:L08708. doi:10.1029/2006GL025779
- Min S-K, Zhang X, Zwiers FW, Hegerl GC (2011) Human contribution to more-intense precipitation extremes. *Nature* 470:378–381
- Min S-K, Son S-W, Seo K-H, Kug J-S, An S-I, Choi Y-S, Jeong J-H, Kim B-M, Kim J-W, Kim Y-H, Lee J-Y, Lee M-I (2015) Changes in weather and climate extremes over Korea and possible causes: a review. *Asia-Pac J Atmos Sci* 51:103–121
- Moss RH, Edmonds JA, Hibbard KA, Manning MR, Steven KR and others (2010) The next generation of scenarios for climate change research and assessment. *Nature* 463:747–756.
- Niu X, Wang S, Tang J, Lee D-K, Gao X, Wu J, Hong S, Gutowski W, McGregor J (2015) Multimodel ensemble projection of precipitation in eastern China under A1B emission scenario. *J Geophys Res Atmos* 120:9965–9980
- Oh SK, Park JH, Lee SH, Suh MS (2014) Assessment of the RegCM4 over East Asia and future precipitation change adapted to the RCP scenarios. *J Geophys Res Atmos* 119:2913–2927
- Park CY, Min SK, Cha DH, Suh MS (2015) Evaluation of multiple regional climate models for summer climate extremes over East Asia. *Clim Dyn*. doi:10.1007/s00382-015-2713-z
- Pfeifer S, Bülow K, Gobiet A, Hänsler A, Mudelsee M, Otto J, Rechid D, Teichmann C, Jacob D (2015) Robustness of ensemble climate projections analyzed with climate signal maps: seasonal and extreme precipitation for Germany. *Atmosphere* 6:677–698. doi:10.3390/atmos6050677
- Raty O, Raisanen J, Ylhäisi JS (2014) Evaluation of delta change and bias correction methods for future daily precipitation: intermodel cross-

- validation using ENSEMBLES simulations. *Clim Dyn* 42:2287–2303
- Sarr MA, Seidou O, Trambly Y, El Adlouni S (2015) Comparison of downscaling methods for mean and extreme precipitation in Senegal. *J Hydrol Reg Stud* 4:369–385
- Seo YA, Lee Y, Park JS, Kim MK, Cho C, Baek HJ (2015) Assessing changes in observed and future projected precipitation extremes in South Korea. *Int J Climatol* 35:1069–1078
- Skamarock WC, Klemp JB, Dudhia J, Gill DO, Duda DMBMG, Huang X-Y, Wang W, Powers JG (2008) A description of the advanced research WRF version 3. NCAR technical note, NCAR/TN-475+STR, 125, doi: [10.5065/D68S4MVH](https://doi.org/10.5065/D68S4MVH).
- Srivastava AK, Delsole T (2014) Robust forced response in south Asian summer monsoon in a future climate. *J Clim* 27:7849–7860
- Sunyer MA, Hundecha Y, Lawrence D, Madenm H, Willems P, Martinkova M, Vormoor K, Biiirger G, Hanel M, Kriauciuniene J, Loukas A, Osuch M, Yiicel I (2015) Inter-comparison of statistical downscaling methods for projection of extreme precipitation in Europe. *Hydrol Earth Syst Sci Discuss* 11:6167–6214
- Sushama L, Laprise R, Caya D, Frigon A, Slivitzky M (2006) Canadian RCM projected climate-change signal and its sensitivity to model errors. *Int J Climatol* 26:2141–2159
- Taylor KE, Stouffer RJ, Meehl GA (2012) An overview of CMIP5 and the experiment design. *Bull Am Meteorol Soc* 93(4):485–498. doi:[10.1175/BAMS-D-11-00094.1](https://doi.org/10.1175/BAMS-D-11-00094.1)
- Tebaldi C, Knutti R (2007) The use of the multi-model ensemble in probabilistic climate projections. *Philos Trans R Soc Lond A Math Phys Eng Sci* 365:2053–2075
- Trenberth KE, Dai A, Rasmussen RM, Parsons DB (2003) The changing character of precipitation. *Bull Am Meteorol Soc* 77:305–324
- Weigel AP, Knutti R, Liniger MA, Appenzeller C (2010) Risks of model weighting in multimodel climate projections. *J Clim* 23:4175–4191
- Willett KM, Gillett NP, Jones PD, Thorne PW (2007) Attribution of observed surface humidity changes to human influence. *Nature* 449:710–712
- Wu J, Gao X-J, Xu Y-L, Pan J (2015) Regional climate change and uncertainty analysis based on four regional climate model simulations over China. *Atmos Oceanic Sci Lett* 8:147–152
- Zhang X, Alexander LV, Hegerl GC, Jones P, Klein Tank A, Peterson TC, Trewin B, Zwiers FW (2011) Indices for monitoring changes in extremes based on daily temperature and precipitation data. *Wiley Interdiscip Rev Clim Chang* 2:851–870. doi:[10.1002/wcc.147](https://doi.org/10.1002/wcc.147)